

First solid-state NMR spectroscopy evaluation of complexes of benznidazole with cyclodextrin derivatives



Josefina Priotti^a, M. João G. Ferreira^b, Maria C. Lamas^{a,c}, Darío Leonardi^{a,c}, Claudio J. Salomon^{a,c}, Teresa G. Nunes^{b,*}

^a IQUIR-CONICET, Suipacha 531, 2000 Rosario, Argentina

^b CQE, Instituto Superior Técnico, Universidade de Lisboa, Av. Rovisco Pais, 1049-001 Lisboa, Portugal

^c Área Técnica Farmacéutica, Facultad de Cs. Bioquímicas y Farmacéuticas, Universidad Nacional de Rosario, Suipacha 531, 2000 Rosario, Argentina

ARTICLE INFO

Article history:

Received 14 March 2015

Received in revised form 7 May 2015

Accepted 22 May 2015

Available online 29 May 2015

ABSTRACT

Complexation of benznidazole (BZL), a drug of choice for the treatment of Chagas' neglected disease, with cyclodextrin (CD) derivatives was analyzed by solid-state NMR. ^{13}C cross polarization/magic angle spinning spectra were recorded from BZL and from BZL: β -CD, BZL:methyl β -CD and BZL:hydroxypropyl β -CD complexes, which were obtained by the solvent evaporation technique. No significant evidence was obtained on BZL inclusion complexes involving either β -CD or hydroxypropyl β -CD. Conversely, BZL:methyl β -CD displayed BZL resonances characteristic of an amorphous drug and data analysis confirmed the presence of stable BZL:methyl β -CD inclusion complexes, with benzene encapsulated into the host cavity. Further evidences on complex structure and dynamics were obtained from proton and carbon spin-lattice relaxation times in the rotating frame. These data are consistent with a common guest-host spin reservoir. The BZL interaction with methyl β -CD provided a route to stabilize amorphous BZL. Physical mixtures with identical BZL and CD compositions were also studied for comparison.

© 2015 Elsevier Ltd. All rights reserved.

1. Introduction

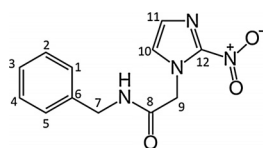
Benznidazole (BZL) (**Scheme 1**), the drug of election for the treatment of Chagas' neglected disease, is classified as class IV by the Biopharmaceutics Classification System (BCS). It is practically insoluble in water (230 $\mu\text{g}/\text{ml}$) and shows poor absorption and fluctuations in plasma levels, leading to a limited oral bioavailability ([Maximiano, Costa, de Sousa, & Cunha-Filho, 2010](#)). According to the available literature, few approaches have been carried out to increase BZL oral bioavailability, including cyclodextrin complexation ([Leonardi, Bombardiere, & Salomon, 2013](#)).

Cyclodextrins (CDs) are a family of natural or synthetically modified cyclic oligosaccharides that have a toroidal shape with lipophilic and hydrophobic inner cavities and a hydrophilic outer surface, on which the hydroxyl groups are located ([Dodziuk, 2008](#); [Loftsson & Duchêne, 2007](#)). They form inclusion complexes with different drugs to enhance its solubility and dissolution rate ([Dodziuk, 2008](#)). Solubilization is enhanced through interaction with water of the OH groups at the surface, while the hydrophobic drug is encapsulated in the apolar inner cavity. The interaction

of BZL with β -cyclodextrin (β -CD), hydroxypropyl- β -cyclodextrin (HP- β -CD) and methyl- β -cyclodextrin (Me- β -CD) has been investigated using differential scanning calorimetry (DSC), scanning electron microscopy (SEM), X-ray diffraction (XRD), phase solubility and dissolution studies. Evidences for complex formation were namely the partial or total disappearance of BZL endothermic peak by DSC in all the prepared samples, loss of crystallinity observed in the different diffractograms and different morphology of the drug particles observed by SEM. Furthermore, higher BZL solubility in water was obtained by CD complexation, in particular for HP- β -CD and Me- β -CD, where the increased hydrophobic nature of the cavity is believed to promote complexation ([Leonardi et al., 2013](#)). Moreover, it was reported that BZL dissolution rate increased as the ratio of carriers increased ([Leonardi et al., 2013; Maximiano, Costa, de Sá Barreto, Bahia, & Cunha-Filho, 2011a](#)), although the end result is also dependent of the method used ([Sobrinho, La Roca Soares, Labandeira, Alves, & Neto, 2011a, 2012](#)). This finding suggested the formation of both inclusion and non-inclusion complexes ([Challa, Ahuja, Ali, & Khar 2005](#)). Molecular modeling was carried out on vacuum in order to determine the more stable BZL conformations in the BZL:CD inclusion complex ([Sobrinho, La Roca Soares, Rolim-Neto, & Torres-Labandeira, 2011b](#)), and the presence of water as solvent was also considered, proving that higher stability was reached in the presence of solvent. However, and despite the

* Corresponding author. Tel.: +351 21 8419043; fax: +351 21 8464455.

E-mail address: teresa.nunes@tecnico.ulisboa.pt (T.G. Nunes).



Scheme 1. Chemical structure of benznidazole (BZL), *N*-benzyl-2-(2-nitro-1*H*-imidazol-1-yl) acetamide.

increasing interest in the development of novel BLZ formulations, as mentioned by World Health Organization (WHO) (2010), NMR data on BZL:CD inclusion complexes are scarce. Solution studies suggest dynamic behavior but only based on differences in chemical shifts observed when comparing the drug and the cyclodextrin to the mixture (Melo et al., 2013; Lyra et al., 2012).

Thus, alternative spectroscopic techniques should be applied to evaluate the molecular structure and physicochemical solid-state properties of BZL by forming inclusion complexes with CD derivatives. In this regard, solid-state NMR has already proved to be a valuable technique to the pharmaceutical industry (Berendt, Sperger, Isbester, & Munson, 2006), e.g. in studies of cyclodextrin inclusion complexes (Potrzebowski & Kazmierski, 2004), as aspartame and neotame into β -cyclodextrin (Garbow, Likos, & Schroeder, 2001) or albendazole into several cyclodextrin derivatives (Ferreira, García, Leonardi, Salomon, Lamas, & Nunes, 2015). To the best of our knowledge, there are no solid-state NMR (ssNMR) reports on these systems. Therefore, the objective of this study is to use ssNMR to obtain evidence for the presence of inclusion complexes without submitting the samples to any previous treatment.

2. Materials and methods

2.1. Materials

BZL (lot 260835, 99.45% purity) was a gift from Produtos Roche Químicos e Farmacéuticos S.A. (Jaguaré, São Paulo, Brazil). β -Cyclodextrin (>99% purity, β -CD), hydroxypropyl- β -cyclodextrin (estimated mol. wt. \approx 1396, average degree of substitution 0.9; purity >98%, HP- β -CD), and methyl- β -cyclodextrin (estimated mol. wt. \approx 1310, average degree of substitution 1.8; purity >98%, Me- β -CD) were purchased from Sigma-Aldrich (Milwaukee, WI, USA). All other chemicals and solvents used in this study were of analytical reagent grade.

2.2. Preparation of the samples

Binary systems of BZL with β -CD, HP- β -CD, and Me- β -CD (1:1 and 1:2 drug:carrier molar ratio) were prepared using the solvent evaporation method. BZL (100 mg) was dissolved in ethanol (10 ml) and CDs in water (10 ml). The solutions were mixed under magnetic stirring (300 rpm) for 10 min. Then, the solvents were evaporated under vacuum (15 mbar) using a rotary flash evaporator (150 rpm) with a water bath at 40 °C. The resulting solid was dried under vacuum for 3 h. After drying, the residue was ground in a mortar and then passed through a 40-mesh metal screen. The resultant powders were stored in a desiccator. Physical mixtures with identical BZL:CD compositions (1:1 and 1:2 drug:carrier molar ratio) were prepared by thoroughly mixing the components in a mortar for 10 min. The resulting residue was dried under vacuum for 2 h and stored overnight in a desiccator. After drying, the residue was ground in a mortar and then passed through a 40-mesh metal screen. The resultant powders were stored in a desiccator until further investigation.

2.3. ^{13}C Solid-state NMR spectroscopy

Powdered samples of BZL and BZL:CDs (\sim 200 mg) were packed into 7 mm o.d. cylindrical zirconia rotors. ^{13}C cross polarization/magic angle spinning (CP/MAS) spectra were obtained at 75.49 MHz on a Tecmag Redstone/Bruker 300 WB spectrometer at a rate of 3.5 kHz with 90° radiofrequency pulses of about 4 μs , contact time of 3 ms and, unless otherwise stated, a relaxation delay of 20 s and 5 s for BZL and BZL:CDs samples, respectively. The significant contributions of the ^{13}C spinning side bands, particularly in the aromatic and carbonyl regions, were eliminated by running the spectra using either the SELTICS sequence (Sideband Elimination by Temporary Interruption of Chemical Shift) (Hong & Harbison, 1993) or the TOSS sequence (TOtal Suppression of Spinning Sidebands) (Dixon, Schaefer, Sefcik, Stejskal, & McKay, 1982). CP/MAS spectra with suppression of ^{13}C non-quaternary signals was achieved by interrupting proton decoupling during 40 μs before the acquisition period. ^{13}C chemical shifts were referenced with respect to external glycine (^{13}CO observed at 176.03 ppm). Deconvolutions of ^{13}C CP/MAS sub-spectra recorded from BZL:Me- β -CD (1:1 and 1:2 drug:carrier molar ratio) were performed using Gaussian functions as the input to obtain the fitting curves by the iterative method of non linear least squares, available in Origin (Microcal Software, Inc., USA). The chemical shifts obtained from crystalline BZL were used as approximate input centroids of the Gaussian curves.

2.3.1. Solid-state NMR relaxation times

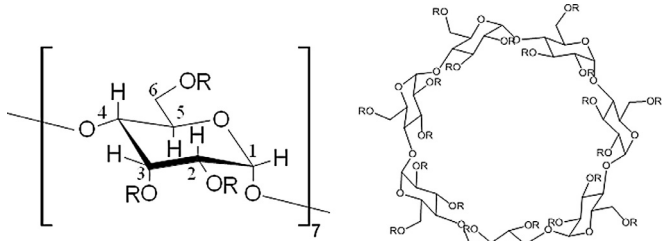
The proton relaxation time in the rotating frame ($^{\text{H}}T_{1\text{p}}$) was measured by recording the carbon signal as a function of the $^{\text{H}}$ spin-locking time in the range 10 μs –26 ms (18 values), before the CP period in ^{13}C CP/MAS experiments. A frequency field of 62.5 kHz was used for the spin-lock field B_1 . The recycle delay was 10 s or 20 s, the number of transients was between 32 and 256 and a contact time of only 400 μs was selected to minimize $^{\text{H}}$ spin-diffusion. The carbon spin-lattice relaxation time in the rotating frame ($^{\text{C}}T_{1\text{p}}$) was measured using a standard CP pulse sequence, with 1 ms contact time, proton spin-locking interruption from 100 μs to 24 ms (12 values) over the cross-polarization period, and 10 s recycle delay. Both $^{\text{H}}T_{1\text{p}}$ and $^{\text{C}}T_{1\text{p}}$ values were determined by the least-squares fit using the experimental data and the exponential function that characterizes the rate of decay of the spin-locked carbon magnetization, $M(t)=M_0\exp(-t/T_{1\text{p}})$, where $M(t)$ is the magnetization at time t , M_0 is the magnetization recorded neither without $^{\text{H}}$ spin-locking time nor with spin-locking interruption previously to the CP period, respectively for $^{\text{H}}T_{1\text{p}}$ and $^{\text{C}}T_{1\text{p}}$ determinations. T_{CH} and $T_{1\text{p}}$ were also obtained from ^{13}C CP/MAS experiments by sequentially increasing the contact time from 10 μs to 20 ms (19 values) and fitting the experimental data to the function $y=(I_0/T_{\text{CH}})((\exp(-t/T_{1\text{p}})-\exp(-t/T_{\text{CH}}))/(1/T_{\text{CH}}-1/T_{1\text{p}}))$, where I_0 is the absolute amplitude and T_{CH} is the time constant for the CP build-up (Kolodziejski & Klinowski, 2002). Relaxation data were always measured at 293 K.

3. Results and discussion

3.1. ^{13}C CP/MAS spectra of cyclodextrins

Scheme 2 shows the structural formula of the β -cyclodextrins evaluated in this study as potential molecules to form BZL inclusion complexes. The hydrogen atoms 3 and 5 are oriented towards the inside of the toroid cavity.

Fig. 1 shows the ^{13}C CP/MAS spectra obtained from β -CD, Me- β -CD and HP- β -CD. The assignment of carbon resonances is shown in **Table 1**. The spectrum of β -CD shows better resolution than the other two. The existence of several signals for each β -CD



Scheme 2. Structural formula of β -cyclodextrins used in this study, where: R=H in β -CD, R= CH_3 in Me- β -CD and R= $\text{CH}_2\text{C}(\text{OH})\text{CH}_3$ in HP- β -CD.

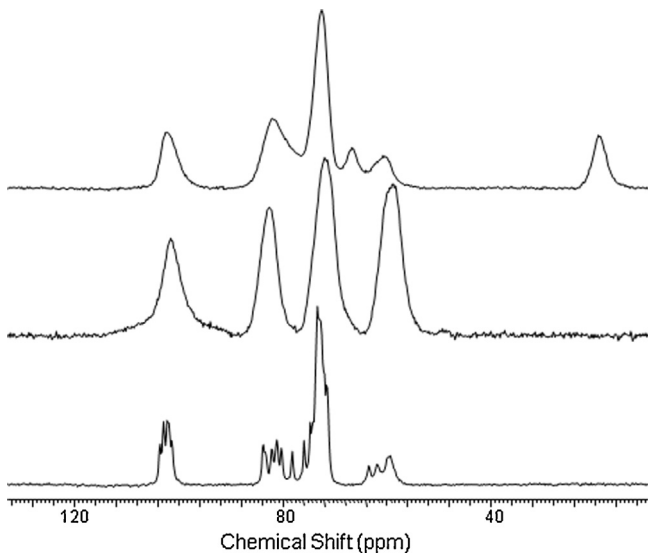


Fig. 1. ^{13}C CP/MAS spectra obtained from β -CD, Me- β -CD and HP- β -CD (from bottom to top).

Table 1

^{13}C CP/MAS chemical shifts (ppm) obtained from β -CD, Me- β -CD and HP- β -CD in pure states.

| Carbon number | β -CD | Me- β -CD | HP- β -CD |
|---|---|-----------------|--|
| 1 | 103.72; 103.03 102.34; 101.48 (102.64) ^a | 101.82 | 102.86 |
| 2,3,5 | 76.05; 74.84 73.45; 71.72 (72.17) ^a | 71.90 | 72.93 |
| 4 | 82.28; 81.24 80.37; 78.30 (81.60) ^a | 82.97 | 81.76 |
| 6 | 63.59; 61.86 61.17; 59.44 (60.77) ^a | 59.44 | 63.94, ^b 60.31 ^b |
| Group substituent | | | |
| $-\text{CH}_3$ | – | 59.44 | – |
| $-\text{OCH}_2\text{C}(\text{OH})\text{CH}_3$ | – | – | ~72, ^b 66.88, 19.31 |

^a Sfih et al. (1996), Wulff, Aldén, and Tegenfeldt (2002).

^b Superimposed.

carbon is due to the variety of torsion angles not only about the (1 \rightarrow 4) linkages for C1 and C4, but also related with the orientation of OH groups (Sfih, Legrand, Doussot, & Guy, 1996, and references therein). On the other hand, the resolution loss in Me- β -CD and HP- β -CD spectra appears to be due to bond distortion, not to conformational change usually leading to larger chemical shift distribution, of about 2.5 to 5 ppm (Inoue, Okuda, & Chûjô, 1985).

3.2. ^{13}C CP/MAS NMR spectra of BZL

Fig. 2 shows a typical ^{13}C CP/MAS spectrum obtained from BZL. At least ten signals are identified. Table 2 presents the chemical shifts of the carbon resonances. Signals from C7, C8 and C9 show small splittings which can be due to ^{13}C dipolar couplings with ^{14}N , a quadrupolar nucleus. Similar interactions may cause other peak broadening (C10, C11 and C12). Overall, a single BZL molecule is assigned here to the asymmetric crystallographic unit because only one resonance was recorded from each carbon species.

The crystal structure of BZL was determined at -173°C (Sobrinho, Cunha, Rolim, Torres-Labandeira, & Dacunha-Marinho, 2008) and at -123°C (Honorio et al., 2014), and only small conformational changes with temperature were reported on the asymmetric unit. The presence of two intramolecular interactions were identified (C9-H9b...ONO and C7-H7b...OC8) which explain the relative orientation of the imidazole group, the benzene group and the central acetamide: the BZL conformation consists in three approximately planar fragments (Honorio et al., 2014). No BZL polymorphs were reported when anti-solvent addition or solvent evaporation were used to promote crystallization (Maximiano, Novack, Bahia, Sá-Barreto, & Cunha-Filho, 2011b). Polymorphs were however prepared from the melt, which exhibited three closely related crystalline forms (Honorio et al., 2014), monotonically related to the most stable one. It was suggested that the polymorphic transformations consist on BZL reorientations enabling the main intermolecular pattern to be conserved (Honorio et al., 2014).

3.3. ^{13}C CP/MAS NMR spectra of solid dispersions of BZL and cyclodextrins

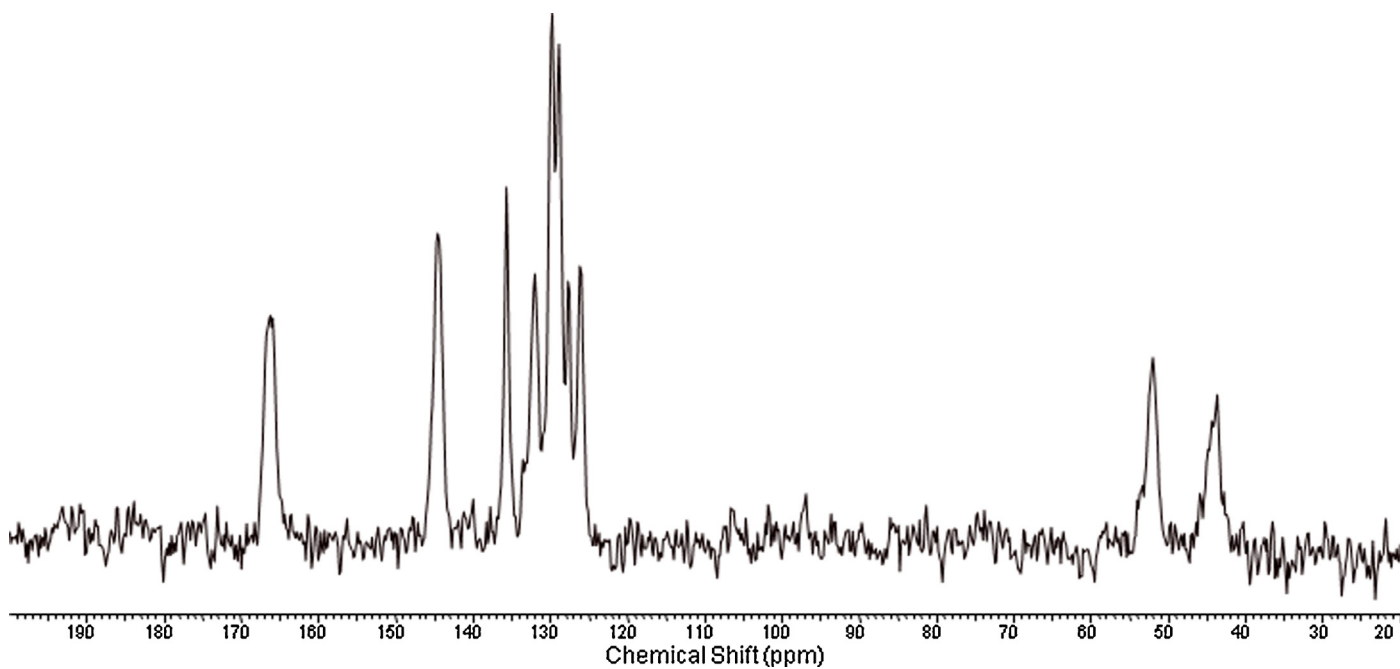
Fig. 3 presents the ^{13}C CP/MAS spectra recorded from BZL: β -CD, BZL:Me- β -CD and BZL:HP- β -CD samples obtained by the solvent evaporation method with host:guest 1:1 molar ratio; the BZL spectrum is also shown for comparison. Although every resonance may be identified, Fig. 3 also displays BZL signals using an expanded vertical scale to help performing a better spectrum analysis. Thus, while BZL and BZL: β -CD signals may be superimposed, BZL:Me- β -CD spectrum shows clearly a loss of resolution, much more severe than in BZL:HP- β -CD spectrum. A similar trend was obtained from BZL: β -CD, BZL:Me- β -CD and BZL:HP- β -CD samples with host:guest 1:2 molar ratio (Fig. 4).

X-ray powder diffraction data reported on BZL:CDs (Leonardi et al., 2013) showed that the loss of crystallinity increased from BZL: β -CD to BZL:HP- β -CD and BZL:Me- β -CD, as observed here using ssNMR. The increased broadening of BZL signals in BZL:Me- β -CD spectrum when compared to pure BZL is consistent with lack of order at short distance, thus to a distribution of resonances as expected for a more amorphous system, strongly suggesting that BZL is encapsulated into the Me- β -CD cavity thus forming an inclusion complex. Moreover, new signals were identified, not observed in the spectrum of pure BZL. Hence, the BZL interaction with Me- β -CD provided a route to stabilize amorphous BZL.

Table 2 shows the ^{13}C CP/MAS chemical shifts obtained from BZL, BZL: β -CD (1:1 and 1:2), BZL:methyl β -CD (1:1 and 1:2) and BZL:hydroxypropyl β -CD (1:1 and 1:2).

The present ssNMR data agrees well with previous DSC analyses (Leonardi et al., 2013). The BZL endothermic peak partial or total disappeared in DSC thermograms obtained from BZL:HP- β -CD and BZL:Me- β -CD, respectively, for both tested drug:carrier molar ratios (1:1 and 1:2). As for BZL: β -CD, the effect was particularly noticed for 1:2 drug:carrier molar ratio.

A more detailed spectral analysis was performed using Gaussian functions for signal deconvolution. Fig. 5 shows ^{13}C CP/MAS

Fig. 2. ^{13}C CP/MAS spectrum obtained from BZL.**Table 2**

^{13}C CP/MAS chemical shifts (ppm) obtained from BZL, BZL: β -CD (1:1 and 1:2), BZL:Me- β -CD (1:1 and 1:2) and BZL:HP- β -CD (1:1 and 1:2). The chemical shifts of BZL:Me- β -CD (1:1 and 1:2) deconvoluted signals depicted in Fig. 5 are shown in bold format.

| Carbon number | BZL | BZL: β -CD | | BZL:Me- β -CD | | BZL:HP- β -CD | |
|---------------|-----------------------------|----------------------------|--------|---|---|------------------------------|--------|
| | | 1:1 | 1:2 | 1:1 | 1:2 | 1:1 | 1:2 |
| 1 | 128.98 | 128.81 | 128.81 | 128.81 128.92 | 128.81 128.80 | 128.98 | 128.98 |
| 2 | 129.84 | 129.84 | 129.84 | 129.84 ^b 130.01 | 129.67 ^b 129.66 | 129.84 | 129.84 |
| 3 | 127.56 | 127.60 | 127.60 | 126.56 ^b 125.94 | 126.56 ^b 126.40 | 127.60 | 127.60 |
| 4 | 129.84 | 129.84 | 129.84 | 129.84 ^b 130.01 | 129.67 ^b 129.66 | 129.84 | 129.84 |
| 5 | 128.98 | 128.81 | 128.81 | 128.81 128.92 | 128.81 128.80 | 128.98 | 128.98 |
| 6 | 135.73 | 135.55 | 135.73 | 135.73 139.36 ^c 135.66 139.14 | 135.73 139.36 ^c 135.67 139.06 | 135.55 138.2 ^c | 135.55 |
| 7 | 52.18 53.73 ^b | 52.18 | 52.0 | 51.66 | 51.48 | 52.18 | 52.18 |
| 8 | 166.34 166.00 | 166.86 166.00 | 166.34 | 166.86 166.49 167.80 | 166.34 ^c 166.35 167.00 | 166.86 166.34 167.04 | 166.17 |
| 9 | 43.87 44.9 ^b | 43.70 44.9 ^b | 43.70 | 43.53 | 43.87 | 44.05 | 44.05 |
| 10 | 132.09 ^a | 132.09 | 131.92 | 132.09 ^b 131.18 | 131.92 ^b 131.09 | 131.92 | 131.92 |
| 11 | 126.04 ^a | 126.04 | 126.04 | 126.04 ^b 127.75 | 126.04 ^b or 127.60 127.89 | 126.04 | 126.04 |
| 12 | 144.38 ^a | 144.72 144.38 | 144.20 | 145.42 146.29 144.85 | 145.93 145.99 144.69 | 144.55 | 144.55 |

^a Broadening due to bond to ^{14}N , a quadrupolar nucleus.

^b Shoulder.

^c Broad.

sub-spectra from BZL:Me- β -CD (1:1 and 1:2 molar ratio) displaying the Gaussian curves used for deconvolution. The chemical shifts of the deconvoluted signals are also shown in Table 2. The resonance at about 139 ppm is tentatively assigned here to C6. Consequently, upon formation of the inclusion complex with Me- β -CD, the C6 signal is observed at higher frequency, with a chemical shift

increase of about 3.5 ppm. This signal is also much broader than the one recorded at about 135 ppm, assigned to C6 in pure BZL (see Figs. 3–5) although it is the BZL best resolved resonance in the spectrum of BZL:Me- β -CD. This signal at 139 ppm could also be assigned to C12, in the imidazole moiety, but this hypothesis would imply a shift of about 5 ppm to lower frequency when

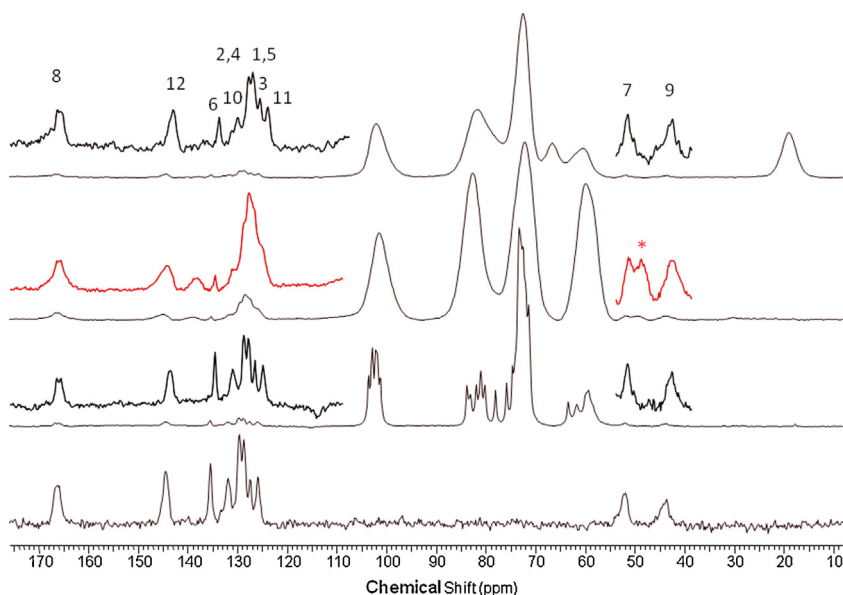


Fig. 3. ^{13}C CP/MAS spectra obtained from BZL and BZL: β -CD, BZL:Me- β -CD and BZL:HP- β -CD (from bottom to top) with 1:1 drug:carrier molar ratio. BZL signals from BZL:CDs are also shown with an expanded vertical scale and BZL:Me- β -CD lines are in red color (for interpretation of the references to color in this figure legend, the reader is referred to the web version of this article). * Denotes Me- β -CD CH_3 signal.

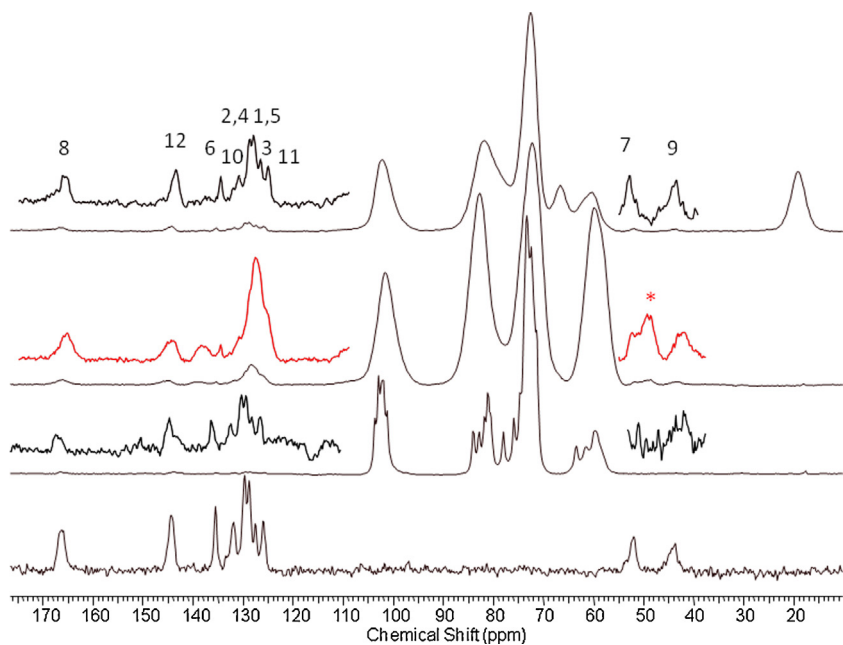


Fig. 4. ^{13}C CP/MAS spectra obtained from BZL and BZL: β -CD, BZL:Me- β -CD and BZL:HP- β -CD (from bottom to top) with 1:2 drug:carrier molar ratio. BZL signals from BZL:CDs are also shown with an expanded vertical scale and BZL:Me- β -CD lines are in red color (for interpretation of the references to color in this figure legend, the reader is referred to the web version of this article). * Denotes Me- β -CD CH_3 signal.

compared to pure BZL, which is ruled out here. Both assignments of the new peak at 139 ppm (to C6 or C12) can only be explained on the basis of a BZL conformational rearrangement in the inclusion complex. Considering that Me- β -CD cavity is apolar, it is reasonable to consider that the benzene ring interaction with the host is favored when compared to the imidazole moiety carrying a polar substituent. Conformational changes will eventually disrupt intramolecular interactions present in the crystalline form (C7—H7b···OC8 or C9—H9b···ONO bond) (Sobrinho et al., 2008); however, subsequent C7 or C9 chemical shift changes are expected to be small and the spectral resolution is not good enough to allow any conclusion.

3.3.1. ^{13}C CP/MAS NMR spectra of physical mixtures of BZL and cyclodextrins

^{13}C CP/MAS spectra were also obtained from physical mixtures prepared with the same molar ratios as the solid dispersions. ^{13}C CP/MAS spectra obtained from BZL and from physical mixtures (PM) of BZL and β -CD, BZL and Me- β -CD, BZL and HP- β -CD (1:1 and 1:2 molar ratio) are provided in the Supplementary data file (Figs. S1 and S2). The spectra were run with acquisition parameters similar to those selected for the observation of the corresponding solid dispersions (Figs. 3 and 4) except for the recycle delay which was 10 s instead of 5 s. That value would enable achieving reasonable spectral signal to noise ratio considering that PMs are

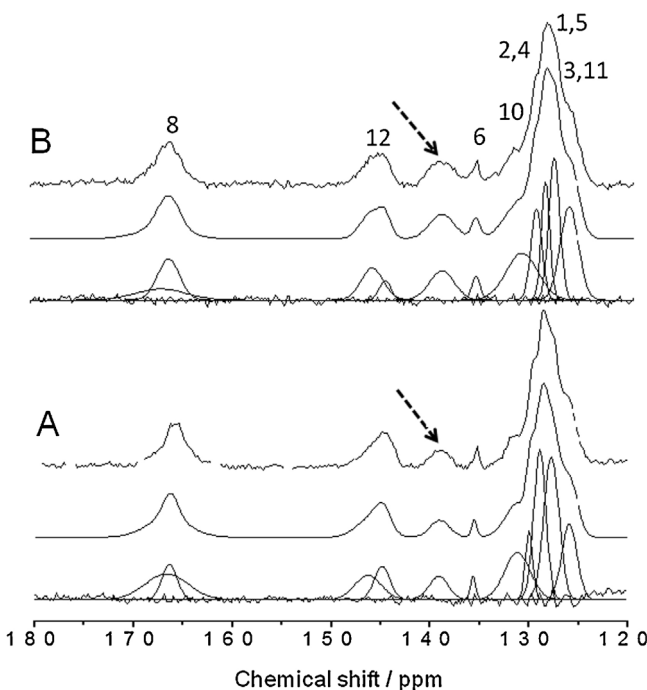


Fig. 5. ^{13}C CP/MAS sub-spectra recorded from BZL:Me- β -CD (A, 1:1) and (B, 1:2) showing (from bottom to top) the Gaussian curves used to deconvolute the isotropic signals and the line fitting residues, and the fitting curve. The arrows indicate the resonances not recorded from pure BZL.

expected to be more rigid systems than solid dispersions (than with longer ^1H spin-lattice relaxation time, parameter that controls the equilibrium magnetization recovery of the spin system in a CP experiment). No spectral evidence was obtained for the presence of inclusion complexes in PMs by comparing Figs. 3 and 4 with Figs. S1 and S2, which just show superimposed BZL and CD resonances obtained separately from each pure compound.

3.4. Proton and carbon spin-lattice relaxation in the rotating frame

The influence of mobility in the relative intensity of the host and guest signals may be probed in the MHz and kHz frequency ranges by measuring the spin-lattice ($^{\text{H}}T_1$ or $^{\text{C}}T_1$) and the spin-locking ($^{\text{H}}T_{1\text{p}}$ or $^{\text{C}}T_{1\text{p}}$) relaxation times, respectively. $^{\text{H}}T_{1\text{p}}$ and $^{\text{C}}T_{1\text{p}}$ are in general much shorter than spin-lattice relaxation times and consequently have limited spin-diffusion contribution. This process is an adiabatic magnetization transfer, whose origin are “flip-flop” transitions between degenerate spin states at a rate that depends on the dipolar ^1H – ^1H coupling. It scales with the inverse of the 6th power of the proton–proton distance and can therefore provide information on the spatial proximity between molecules. Interpretation of relaxation data based on molecular mobility requires evaluating relaxation under experimental conditions which minimize the spin-diffusion process that may act as an alternative relaxation mechanism.

Motion is the driving mechanism for $^{\text{C}}T_{1\text{p}}$, particularly in amorphous compounds because it is less influenced by spin-diffusion than $^{\text{H}}T_{1\text{p}}$ due to the fact that the spin-diffusion rate increases with magnetogyric ratio and natural isotopic abundance (and is therefore higher for ^1H than ^{13}C). Moreover, $^{\text{C}}T_{1\text{p}}$ allows each carbon to be probed separately and provides information on local mobility. Local dynamics probed by $^{\text{C}}T_{1\text{p}}$ is the random orientational motion of dipolar-coupled C–H nuclei occurring at the rotating-frame Larmor frequency (Koenig, 1999), which in the present study was about 62 kHz (frequency field used for the spin-lock field B_1).

Considering that the BZL:Me- β -CD solid dispersions presented the most clear ^{13}C CP/MAS spectral evidences for the presence of inclusion complexes, additional information was obtained from relaxation measurements because significantly different mobility is expected between free and complexed molecules. Formation of a BZL inclusion complex with Me- β -CD is expected also to favor spin-diffusion because shorter intermolecular distance separates the guest from the host. Preliminary ^{13}C MAS spectra were recorded from BZL:Me- β -CD with 1:1 drug:carrier molar under various experimental conditions to evaluate which relaxation time would best probe those effects. Based on these results (see Figs. S3–S5 in Supplementary data) $^{\text{H}}T_{1\text{p}}$ and $^{\text{C}}T_{1\text{p}}$ were chosen to probe spin-diffusion and mobility, respectively. The time constants for the ^{13}C magnetization build-up under CP (T_{CH}) were also obtained, as well as $T_{1\text{p}}$ which include relaxation contributions from both proton and carbon nuclei (Hediger, Emsley, & Fischer, 1999).

As an illustration, Fig. 6 shows the magnetization decays obtained from BZL:Me- β -CD (1:1) which were used to fit first order exponential functions to obtain $^{\text{H}}T_{1\text{p}}$ and $^{\text{C}}T_{1\text{p}}$ data of the indicated nuclei. BZL relaxation times were measured using the signal with the highest intensity, recorded at about 129 ppm and with dominant contributions assigned to C1,2,4,5 in the benzene ring. An example of the magnetization variation with CP contact time obtained from ^{13}C CP/MAS spectra is displayed in Fig. S6 (Supplementary data). Table 3 shows the relaxation data obtained for free and complexed Me- β -CD and BZL, respectively.

The most significant results and conclusions are:

- (a) Similar $^{\text{H}}T_{1\text{p}}$ data were measured for Me- β -CD, both in pure state and as an inclusion complex host (about 11 ms). Such result indicates that, due to spin-diffusion, all the protons are part of a single spin reservoir and that BZL inclusion did not significantly change Me- β -CD mobility. As mentioned before, for highly dipolar coupled nuclei as protons, spin-diffusion can be the driven relaxation mechanism and can prevail over motional processes.
- (b) $^{\text{H}}T_{1\text{p}}$ data obtained for BZL: > 300 ms in pure state and 14.2 ± 4.3 ms in the BZL:Me- β -CD (1:1) complex. Concerning pure BZL, long $^{\text{H}}T_{1\text{p}}$ and, presumably, $^{\text{H}}T_1$ (hence the selected 20 s recycle delay indicated in Section 2.3.1.). Solid-State NMR relaxation times are consistent with very restricted motion both in the kHz and in the MHz frequency ranges, spin-diffusion being then the alternative relaxation mechanism. However, BZL $^{\text{H}}T_{1\text{p}}$ has strongly decreased in BZL:Me- β -CD, and BZL and Me- β -CD have similar $^{\text{H}}T_{1\text{p}}$ values, which clearly suggests a common spin reservoir, with guest–host smaller ^1H – ^1H distances favoring spin-diffusion, thus giving further evidence for the presence of an inclusion complex. It must be pointed out here that it would have been more correct to compare the inclusion complex $^{\text{H}}T_{1\text{p}}$ data to $^{\text{H}}T_{1\text{p}}$ values from pure amorphous BZL. However, it was impossible to perform the necessary relaxation study because amorphous BZL is very unstable (based on hot-stage microscopy and DSC observations, it was reported on BZL recrystallization subsequent to fast quenching from melted samples) (Honarato et al., 2014). On the other hand, ssNMR spectra and previous XRD data (Leonardi et al., 2013) from solid dispersions obtained by solvent evaporation show that BZL amorphization occurred and that the amorphous form is stable over long periods of time. This observation strongly suggests that BZL interacts with Me- β -CD and that such interaction is capable of stabilizing amorphous BZL.
- (c) $^{\text{C}}T_{1\text{p}}$ obtained for C1,2,4,5 in BZL benzene ring (7.5 ± 0.8 ms) for the sample BZL:Me- β -CD (1:1) is consistent with less restricted molecular motion for the guest than for the host, in which case $^{\text{C}}T_{1\text{p}}$ data exceeded 12 ms. T_{CH} data of Me- β -CD point to more mobility involving C1, C4 and C2,3,5 in the complex than in pure

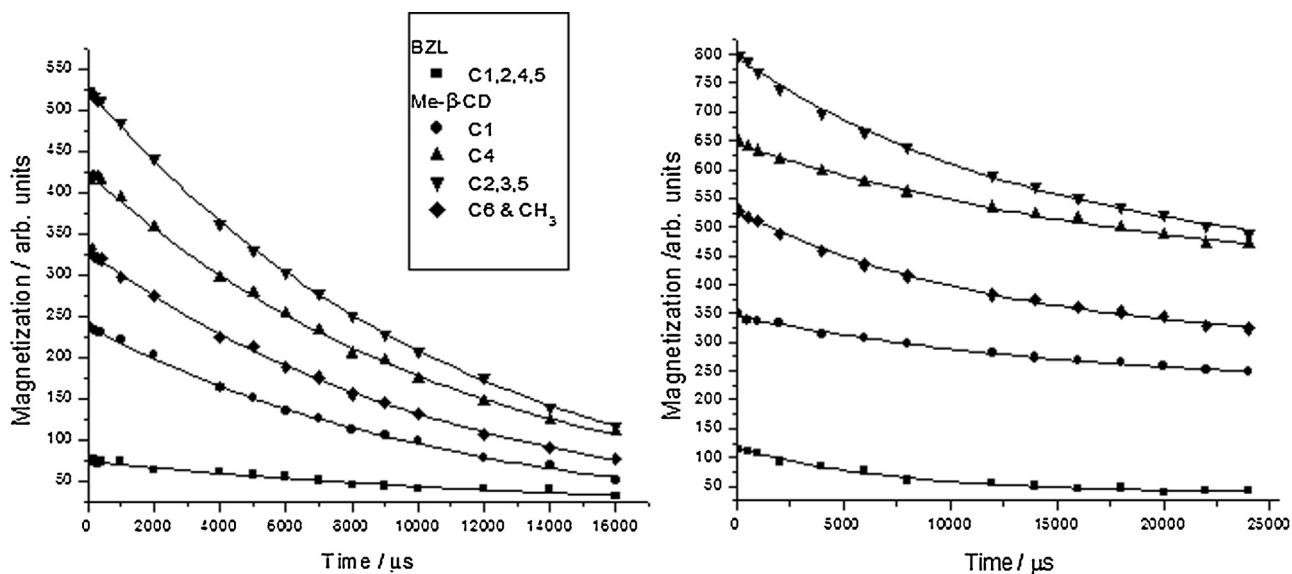


Fig. 6. Magnetization decays with time obtained from ^{13}C CP/MAS of BZL:Me- β -CD to determine $^{\text{H}}T_{1\text{p}}$ (left plot) and $^{\text{C}}T_{1\text{p}}$ (right plot) of the indicated carbon nuclei (see Section 2.3.1. for details). The curves represent first order exponential decay functions from least-squares fits. Magnetization (arb. units) was the highest intensity of the assigned peaks divided here by 1000.

Table 3

Proton and carbon spin-lattice relaxation time in the rotating frame ($^{\text{H}}T_{1\text{p}}$, $^{\text{C}}T_{1\text{p}}$ and $T_{1\text{p}}$) and time constants for the ^{13}C magnetization build-up under CP (T_{CH}), obtained for a) methyl β -CD and b) BZL:Me- β -CD (1:1) complex.

| a) | | | | |
|---------------------|---------------------------------|----------------------|----------------------|---------------------------------|
| Me- β -CD | | | | |
| Carbon number | $^{\text{C}}T_{1\text{p}}$ (ms) | $T_{1\text{p}}$ (ms) | T_{CH} (μs) | $^{\text{H}}T_{1\text{p}}$ (ms) |
| 1 | 14 ± 9 | 13.7 ± 1.0 | 50.8 ± 5.2 | 9.8 ± 1.0 |
| 4 | 9.9 ± 3.1 | 14.2 ± 1.4 | 51.5 ± 6.2 | 10.8 ± 1.5 |
| 2,3,5 | 14.2 ± 3.7 | 14.6 ± 1.6 | 43.1 ± 5.8 | 11.6 ± 0.8 |
| 6 & CH ₃ | 6.2 ± 1.9 | 14.5 ± 1.6 | 132.7 ± 15.6 | 9.8 ± 1.3 |

| b) | | | | |
|---------------------------|------------|------------|--------------|------------|
| BZL:Me- β -CD (1:1) | | | | |
| BZL | | | | |
| 1,2,4,5 | 7.5 ± 0.8 | 18.1 ± 1.5 | 113.5 ± 15.1 | 14.2 ± 4.3 |
| Me- β -CD | | | | |
| 1 | 16.3 ± 2.0 | 11.8 ± 0.8 | 83.9 ± 9.8 | 11.2 ± 0.7 |
| 4 | 20.5 ± 2.4 | 12.3 ± 0.7 | 82.2 ± 8.5 | 11.3 ± 0.7 |
| 2,3,5 | 14.3 ± 1.1 | 11.9 ± 0.6 | 71.8 ± 7.4 | 11.4 ± 0.3 |
| 6 & CH ₃ | 12.4 ± 0.9 | 12.7 ± 0.9 | 135.6 ± 16.6 | 10.9 ± 0.5 |

Me- β -CD; BZL value ($113.5 \pm 15.1 \mu\text{s}$) is comparable to C6 and CH₃ data, although referring to carbons with different multiplicities.

It is worth mentioning that further structural elucidation on BZL:CD inclusion complexes could be obtained from ssNMR experiments using techniques that generally require higher magnetic fields and fast MAS. For example, 2D heteronuclear and homonuclear correlation experiments involving ^1H , ^{13}C and other NMR active nuclei were used to reveal the inclusion of drug inside the CD cavity in a collection of powder samples (Vogt & Strohmeier, 2012).

Future work will include the evaluation of the long term stability of the BZL:Me- β -CD inclusion complex. This study will be performed by measuring $^{\text{C}}T_{1\text{p}}$ as a function of temperature to obtain evidence for local motions in the kHz frequency scale as dynamic heterogeneity is essential for the stability of an amorphous form, as recently reported for example on simvastatin, a cholesterol-lowering agent (Nunes et al., 2014).

4. Conclusions

^{13}C CP/MAS data are consistent with the formation of an inclusion complex BZL:Me- β -CD, with the benzene ring encapsulated into the apolar CD cavity in a different conformation from the one in the crystal structure. An interaction between the benzene ring and the Me- β -CD cavity should be favored, with the imidazole ring interacting with the hydroxyl groups outside the host macrocycle hollow. The confirmation of the inclusion complex between BZL and Me- β -CD is based on the analysis of the differences in the chemical shifts and modification of the peaks between the free and complexed guest molecules. The appearance of a new signal at about 139 ppm, the split up into two resonances for atoms C12 and the peak broadening indicate the occurrence of an inclusion complex and coexistence of different BZL structural arrangements. Further evidences for the presence of the inclusion complex were obtained from proton and carbon spin-lattice relaxation in the rotating frame, which were consistent with a common guest-host spin reservoir and higher mobility in the kHz frequency range for the guest than for the host, respectively. No relevant spectral observation was obtained on the presence of BZL inclusion complexes involving either β -CD or HP- β -CD. The present ssNMR results agree well with earlier published data using other techniques like DSC and X-ray diffraction. The interaction with Me- β -CD provides a route to stabilize amorphous BZL.

Acknowledgement

This work has been carried out with financial support from UNR (Argentina), CONICET (Argentina) and "Fundação para Ciência e Tecnologia" (FCT, Portugal, project RECI/QEQ-QIN/0189/2012). J.P. also acknowledges CONICET for a Ph D fellowship.

Appendix A. Supplementary data

Supplementary data associated with this article can be found, in the online version, at <http://dx.doi.org/10.1016/j.carbpol.2015.05.045>

References

- Berendt, R. T., Sperger, D. M., Isbester, P. K., & Munson, E. J. (2006). Solid-state NMR spectroscopy in pharmaceutical research and analysis. *TrAC Trends in Analytical Chemistry*, 25(10), 977–984.
- Challa, R., Ahuja, A., Ali, J., & Khar, R. K. (2005). Cyclodextrins in drug delivery: An updated review. *AAPS PharmSciTech*, 6, E329–E357.
- Dixon, W. T., Schaefer, J., Sevcik, M. D., Stejskal, E. O., & McKay, R. A. (1982). Total suppression of spinning sidebands in CPMAS C-13 NMR. *Journal of Magnetic Resonance*, 49, 341–345.
- Dodziuk, H. (2008). Molecules with holes-cyclodextrins. In D. Helena (Ed.), *In cyclodextrins and their complexes*. Weinheim: Wiley-VCH Verlag GmbH & Co. KGaA.
- Ferreira, M. J., García, A., Leonardi, D., Salomon, C. J., Lamas, M. C., & Nunes, T. G. (2015). ^{13}C and ^{15}N solid-state NMR studies on albendazole and cyclodextrin albendazole complexes. *Carbohydrate Polymers*, 123, 130–135.
- Garbow, J. R., Likos, J. J., & Schroeder, S. A. (2001). Structure, dynamics, and stability of β -cyclodextrin inclusion complexes of aspartame and neutame. *Journal of Agricultural and Food Chemistry*, 49, 2053–2060.
- Hediger, S., Emsley, L., & Fischer, M. (1999). Solid-state NMR characterization of hydration effects on polymer mobility in onion cell-wall material. *Carbohydrate Research*, 322, 102–112.
- Hong, J., & Harbison, G. (1993). Sideband elimination by temporary interruption of chemical shift. *Journal of Magnetic Resonance Series A*, 105, 128–136.
- Honorato, S. B., Mendonça, J. S., Boechat, N., Oliveira, A. C., Filho, J. M., Ellena, J., et al. (2014). Novel polymorphs of the anti-trypanosoma cruzi drug benzimidazole. *Spectrochimica Acta A: Molecular and Biomolecular Spectroscopy*, 118, 389–394.
- Inoue, Y., Okuda, T., & Chūjō, R. (1985). A high-resolution c.p.-m.a.s. ^{13}C -n.m.r. study of solid-state cyclomaltohexaose inclusion-complexes: Chemical shifts and structure of the host cyclomaltohexaose. *Carbohydrate Research*, 141, 179–190.
- Koenig, J. L. (1999). *In spectroscopy of polymers* (2nd ed., pp. 397–440). Amsterdam, the Netherlands: Elsevier Science.
- Kolodziejski, W., & Klinowski, J. (2002). Kinetics of cross-polarization in solid-state NMR: A guide for chemists. *Chemical Reviews*, 102, 613–628.
- Leonardi, D., Bombardiere, M. E., & Salomon, C. J. (2013). Effects of benzimidazole:cyclodextrin complexes on the drug bioavailability upon oral administration to rats. *International Journal of Biological Macromolecules*, 62, 543–548.
- Loftsson, T., & Duchêne, D. (2007). Cyclodextrins and their pharmaceutical applications. *International Journal of Pharmaceutics*, 329, 1–11.
- Lyra, M. A. M., Soares-Sobrinho, J. L., Figueiredo, R. C. B. Q., Sandes, J. M., Lima, A. A. N., Tenório, R. P., et al. (2012). Study of benzimidazole-cyclodextrin inclusion complexes, cytotoxicity and trypanocidal activity. *Journal of Inclusion Phenomena and Macroyclic Chemistry*, 73, 397–404.
- Maximiano, F. P., Costa, G. H., de Souza, J., & Cunha-Filho, M. S. S. (2010). Caracterização físico-química do fármaco antichagásico benzimidazol. *Química Nova*, 33, 1714–1719.
- Maximiano, F. P., Costa, G. H., de Sá Barreto, L. C., Bahia, M. T., & Cunha-Filho, M. S. (2011). Development of effervescent tablets containing benzimidazole complexed with cyclodextrin. *Journal of Pharmacy and Pharmacology*, 63, 786–793.
- Maximiano, F. P., Novack, K. M., Bahia, M. T., Sá-Barreto, L. L., & Cunha-Filho, M. S. (2011). Polymorphic screen and drug-excipient compatibility studies of the antichagasic benzimidazole. *Journal of Thermal Analysis and Calorimetry*, 106, 819–824.
- Melo, P. N., Barbosa, E. G., Caland, L. B., Carpegianni, H., Garnero, C., Longhi, M., et al. (2013). Host-guest interactions between benzimidazole and beta-cyclodextrin in multicomponent complex systems involving hydrophilic polymers and triethanolamine in aqueous solution. *Journal of Molecular Liquids*, 186, 147–150.
- Nunes, T. G., Viciosa, M. T., Correia, N. T., Danède, F., Nunes, R. G., & Diogo, H. P. (2014). A stable amorphous statin: Solid-state NMR and dielectric studies on dynamic heterogeneity of simvastatin. *Molecular Pharmaceutics*, 11, 727–737.
- Potrzebowski, M. J., & Kazmierski, S. (2004). High-resolution solid-state NMR studies of inclusion complexes. In J. Klinowski (Ed.), *New techniques in solid-state NMR, Top. Curr. Chem.* (246) (pp. 91–140). Berlin, Heidelberg: Springer.
- Sfihi, H., Legrand, A. P., Doussot, J., & Guy, A. (1996). Solid-state ^{13}C NMR study of β -cyclodextrin/substituted aromatic ketone complexes: Evidence for two kinds of complexation of the guest molecules. *Colloids and Surfaces A: Physicochemical and Engineering Aspects*, 115, 115–126.
- Sobrinho, J. L. S., Cunha, M. L. S. S., Rolim, P. J., Torres-Labandeira, J. J., & Dacunha-Marinho, B. (2008). Benzimidazole. *Acta Crystallographica Section E Structure Reports Online*, 64, O634–U1512.
- Sobrinho, J. L. S., La Roca Soares, M. F., Rolim-Neto, P. J., & Torres-Labandeira, J. J. (2011). Physicochemical study of solid-state benzimidazole-cyclodextrin complexes. *Journal of Thermal Analysis and Calorimetry*, 106, 319–325.
- Sobrinho, J. L. S., La Roca Soares, M. F., Labandeira, J. J. T., Alves, L. D. S., & Neto, P. J. R. (2011). Improving the solubility of the antichagasic drug benzimidazole through formation of inclusion complexes with cyclodextrins. *Química Nova*, 34(9), 1534–1538.
- Sobrinho, J. L. S., Santos, F. L. A., Lyra, M. A. M., Alves, L. D. S., Rolim, L. A., Lima, A. A. N., et al. (2012). Benzimidazole drug delivery by binary and multicomponent inclusion complexes using cyclodextrins and polymers. *Carbohydrate Polymers*, 89, 323–330.
- Vogt, F. G., & Strohmeier, M. (2012). 2D solid-state NMR analysis of inclusion in drug-cyclodextrin complexes. *Molecular Pharmaceutics*, 9, 3357–3374.
- World Health Organization (WHO). (2010). Working to overcome the global impact of neglected tropical diseases. In *First WHO report on neglected tropical diseases*. WHO.
- Wulff, M., Aldén, M., & Tegenfeldt, J. (2002). Solid-state NMR investigation of indo-methacin-cyclodextrin complexes in PEG6000 carrier. *Bioconjugate Chemistry*, 13, 240–248.